Designing a spherical microphone array for the directional analysis of reflections and reverberation

Gover, B. N.; Ryan, J. G.; Stinson, M. R.

Publisher's version / Version de l'éditeur:

Audio Engineering Society 115th Convention [Proceedings], pp. 1-11, 2003-10-01

Designing a spherical microphone array for the directional analysis of reflections and reverberation

Gover, B.N.; Ryan, J.G.; Stinson, M.R.

NRCC-46626

A version of this document is published in / Une version de ce document se trouve dans :
Audio Engineering Society, 115th Convention, New York, NY.,
Oct. 10-13, 2003, pp. 1-11

Audio Engineering Society
Convention Paper
Presented at the 115th Convention
2003 October 10–13 New York, NY, USA

Designing a spherical microphone array for the directional analysis of reflections and reverberation

Bradford N. Gover[1], James G. Ryan[2], and Michael R. Stinson[3]

[1] *Institute for Research in Construction, National Research Council, Ottawa, Ontario K1A 0R6, Canada*

[2] *Gennum Corporation, 232 Herzberg Rd., Kanata, Ontario, K2K 2A1, Canada*

[3] *Institute for Microstructural Sciences, National Research Council, Ottawa, Ontario K1A 0R6, Canada*

Correspondence should be addressed to Bradford N. Gover (brad.gover@nrc-cnrc.gc.ca)

ABSTRACT

Spherical microphone array designs were investigated from the point of view of suitability for directional analysis of reverberant sound fields. Four array geometries (tetrahedron, cube, dodecahedron, geodesic sphere) were considered. Beamforming filters were designed using a constrained gain maximization process. The theoretical performance of each array was then predicted. A room acoustic simulator was used to help assess sufficient directionality and evaluate the suitability of each design. A 32-element geodesic sphere array was constructed and used to make directional measurements in real sound fields.

1. INTRODUCTION

Measurement of directional information in a sound field is frequently of great interest. "Directional information" is meant to refer to characteristics of the angular distribution of sound passing through a point. Such information is not readily available through observation of the pressure or intensity alone. The sound pressure is a non-directional measure, whereas intensity is a vector indicating the net direction of energy flow, not necessarily the direction of arrival of component sound waves. Application areas in which knowledge of directional properties of sound fields could be useful include room acoustic analysis and characterization [1, 2, 3] psychoacoustic assessment of halls [4, 5, 6, 7], or localization of sources and reflections [8, 9, 10], to name just a few.

A straightforward approach at obtaining directional information is to employ a detector that is responsive to sounds arriving from one direction only. A directional detector could mean a single directional transducer, a shotgun microphone, a parabolic microphone [1], or a microphone array [2, 8, 11, 12], for instance. Performance issues (such as angular resolution, bandwidth, fidelity) and practical issues (such as ease of steering in different directions, size, cost) together dictate what type of detector is desirable.

Beamforming microphone arrays have many favourable properties for directional pickup of sound. They can be designed to yield high directionality, a broad frequency range of operation, and can be steered electronically in many directions simultaneously, without the need for movement of the array. With modern electret microphones and digital acquisition hardware, highly sophisticated arrays can be realized quite inexpensively.

Choice of suitable array geometry is an issue. If the goal is to design a directional detector for analyzing sound fields (as in the present work), then in many instances one desirable attribute is spherical symmetry. A spherical array can enable steering an identical beam in any three-dimensional direction. Linear or planar arrays do not.

This paper outlines the steps taken in the design of a spherical microphone array intended for directional analysis of sound fields. A design is selected and constructed, and directional measurements are performed.

2. DIRECTIONALITY REQUIREMENTS

The directional resolution of an array is not infinite. The response pattern (beam pattern) usually will have peak sensitivity in the steering direction, with sensitivity rolling off away from this direction. The breadth of this main lobe and steepness of the roll off, as well as the level of any sidelobes all contribute to the overall angular discrimination capabilities. Two common measures used to quantify this

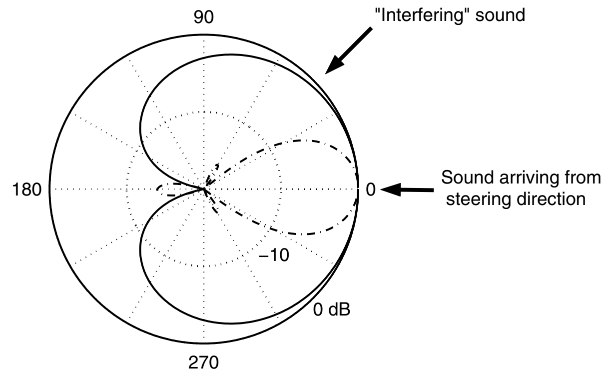

Fig. 1: Illustration of importance of beamwidth for resolving incident sound. The "Interfering" sound will be detected strongly by the cardioid (solid curve), but largely rejected by the fourth-order hypercardioid (broken curve).

are the 3 dB-beamwidth and the directivity index, DI. The 3 dB-beamwidth is the angular width between the half-power points on the main lobe, while the directivity index is the peak-to-average ratio of the beam pattern, expressed in decibels.

The question of how narrow a beam can be realized will be addressed in the next section. This section will address the issue of how narrow a beam is required to obtain useful information from a sound field.

In a free field, the notion of sufficient directionality is easily envisioned. For instance, if two sound waves of interest are incident from two closely-spaced directions, to resolve them a beam has to be narrow enough that only one is sensed at a time. That is, the beamwidth must be less than the angular separation between them. See Fig. 1. In the figure, the first-order cardioid pattern (solid curve) is not narrow enough to resolve the two arrivals, whereas the fourth-order hypercardioid is. (The term "n^{th}-order hypercardioid" refers to the beam of n^{th}-order which maximizes the directivity index [13].)

In an enclosure, sound is sure to arrive not only from discrete directions, but eventually from all directions. In this case it is not obvious how narrow a beam is necessary to reveal detail in the measured pattern.

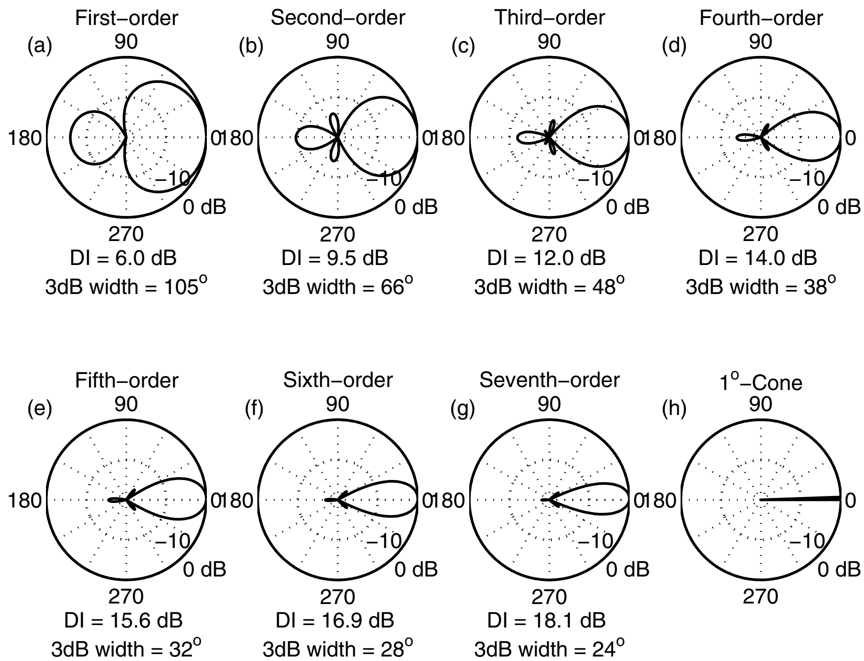

Fig. 2: Receiver beam patterns used in room simulator: (a)–(g) first 7 orders of hypercardioid, and (h) a 1°-wide cone.

To examine this issue, a method of images room simulator derived from one described in Ref. [14] was used. The receiver in the simulator can be assigned one of several directivity patterns, and can be steered in any direction. Each image source contribution to the impulse response is scaled by the microphone directivity in its direction. In this way, a directional impulse response can be obtained in any number of directions at the receiving position. By computing the energy in each response, the pattern of arriving energy with direction is determined. If the beamwidth is too large, the details of the pattern will be smoothed out. The limiting case is of a "pencil beam" receiver, which is also simulated for comparison. (Note that the "energy" is not necessarily the net acoustic field energy, but rather the energy which would be transported towards the detector by a plane wave whose pressure is given by the impulse response.)

The receiver patterns used in the simulator are shown in Fig. 2. Panels (a)–(g) are for the first 7 orders of hypercardioid microphones [13], panel (h) is the pencil beam—a "brick-wall" cone, 1° wide. Note that there are prohibitive noise and construction issues which make it difficult, if not impossible, at the moment to construct transducers with directivities corresponding to the third-order and higher patterns [13].

Results for the simulation of a small rectangular room are shown in Fig. 3. The plots show the energy arriving at the receiver position, in a plane parallel to the floor. The room had dimensions $L_X = 4.65$ m, $L_Y = 6.70$ m, $L_Z = 2.44$ m and had reflection coefficients of 0.75 for each surface. The source was located at ($X_S = 2.77$ m, $Y_S = 4.51$ m, $Z_S = 1.02$ m) and the receiver at ($X_R = 1.58$ m, $Y_R = 4.47$ m, $Z_R = 1.04$ m). This arrangement yields a strong "flutter echo" component propagating back and forth along 0°–180° axis. The direct sound arrival has been removed from the responses.

The pattern received with the 1°-cone can be thought of, in a sense, as the "correct answer" (insofar as the angular quantization is 1°). The other patterns are basically convolutions of this with the individual beam patterns. Notice that for orders up to about third, no detail to speak of is visible. In

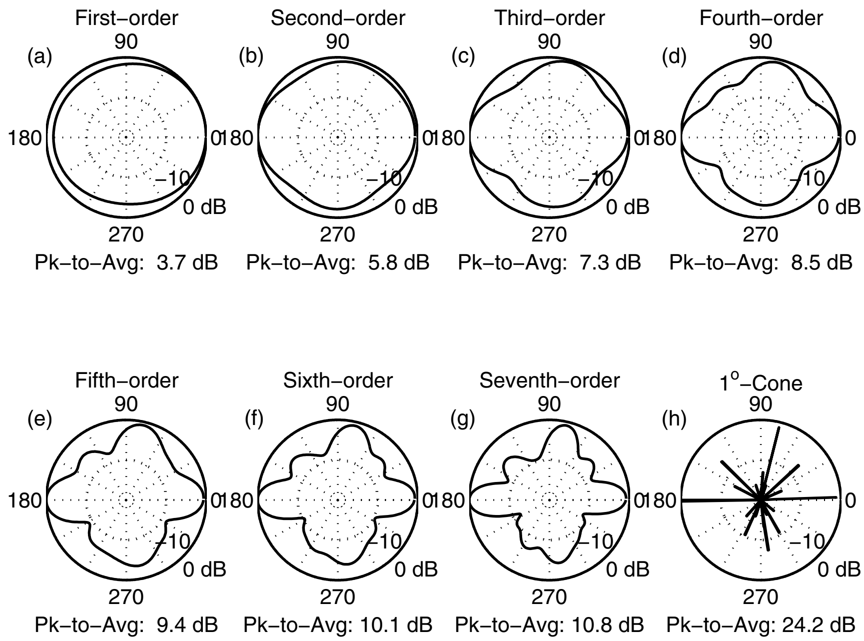

Fig. 3: Simulated received energy patterns for first 7 orders of hypercardioid, and 1°-cone receiver. Energy arriving at the receiver position, in a plane parallel to the floor of a simulated rectangular room. The direct arrival has been removed.

the third order and higher patterns, the flutter echo is discernible. Around fourth or fifth order, it appears that detail in the energy arriving between the big peaks emerges. These qualitative statements essentially amount to noticing that "more detail is resolvable with a narrower pattern", an observation which is supported by the peak-to-average ratios of received energy, indicated in the figure. A higher value indicates a more directional measurement, and it can be seen that the numbers increase as the patterns qualitatively appear to contain more detail. There is a "point of diminishing returns". Above fifth order, the peak-to-average ratio increases only by 0.7 dB per order. The increases per order are larger for the lower orders, up to fourth.

So it seems, (from this one example, at least) that if a design can only achieve second or third-order performance, some information (such as the peak at 135°) will not be discernible. This line of reasoning leads to a beamforming design "target" of directivity index at least 14 dB, beamwidth of at most 38°.

3. BEAMFORMER DESIGN

As mentioned above, to design a beamforming microphone array, both the geometry and the array weights must be determined. Having a design target in mind, proposed designs can be evaluated as to suitability. The process followed herein is exactly that: a geometry is conceived, beamforming weights are designed, and the beamformer performance is predicted and assessed in light of the target.

3.1. Beamforming Procedure

Beamformer design has developed extensively in the past 50 years or so; discussions can be found in textbooks such as Ref. [15]. Delay-and-sum designs are simple and robust, but only provide maximum directional gain over a narrow frequency range [16, 17]. Superdirective approaches can achieve higher directional gain over a wider frequency range, but at the expense of simplicity and robustness [13, 18]. The signal-to-noise ratio becomes a problem at low frequencies, where the phase change of the sound waves is small over the spatial extent of the array. At higher frequencies, the wavelengths become shorter than the intermicrophone spacing, causing problems with spatial aliasing. General tradeoffs in achieving higher directionality over a broader frequency range include: tighter required microphone tolerances, less noise immunity, and possibly more difficult construction issues.

The beamformer design procedure used in this work circumvents some of the common noise-induced frequency-restrictive issues to yield a beam which retains a high directionality over a fairly broad frequency range. The procedure is described in Ref. [19], and is outlined in Ref. [12]. It is an optimized filter-and-sum approach, types of which are discussed in Refs. [18, 20, 21].

For an array with weights $\mathbf{w}$, the directional gain $G(\omega)$ at frequency ω is given by

$$G(\omega) = \frac{\mathbf{w}^H \mathbf{R}_{SS} \mathbf{w}}{\mathbf{w}^H \mathbf{R}_{NN} \mathbf{w}}, \tag{1}$$

where $\mathbf{R}_{SS}$ is the signal correlation matrix, and $\mathbf{R}_{NN}$ is the noise correlation matrix, and the superscript H indicates Hermitian transpose. This quantity gives the signal-to-noise improvement using the array, as compared to that using a single microphone.

For spatially-white noise, the noise correlation matrix becomes the identity matrix, and the expression for the directional gain reduces to

$$G_w(\omega) = \frac{\mathbf{w}^H \mathbf{R}_{SS} \mathbf{w}}{\mathbf{w}^H \mathbf{w}}, \tag{2}$$

which is the white noise gain. The white noise gain gives a measure of the ability of the array to reject uncorrelated noise. High white noise gain means high robustness, and vice versa.

For a given array geometry, it can be seen that the directional gain depends on the microphone signals (determined by steering direction), the noise field, and the array weights. The task is to best select the array weights. Essentially, the present approach assumes a level of noise and microphone mismatch, and incorporates these factors into the estimate of the noise correlation matrix. Then, maximization of the array gain results in a beamformer design which is simultaneously robust and gain-maximized. That is, it is a constrained optimization technique, the constraint being on the white noise gain.

Notwithstanding the details of the design, in the present context, the procedure was used as a "black box" process. Taking a proposed array geometry, steering direction, and microphone mismatch as input, the design process outputs the beamforming filters, as well as the directional gain and white noise gain versus frequency. Both of these metrics can be used in assessing the design's performance.

3.2. Beams for Different Spherical Geometries

Design results for a tetrahedral array (4 microphones) are shown in Fig. 4. Those for a cubic array (8 microphones) are shown Fig. 5, and those for a dodecahedral array (20 microphones) are in Fig. 6. These are all regular polyhedra, possessing high degrees of symmetry. An additional geometry considered is a non-regular polyhedron—a geodesic sphere. The results for a geodesic sphere array (32 microphones) are shown in Fig. 7.

Each of Figs. 4–7 has the same layout: Panel (a) shows the geometry of the array. All arrays were designed to have a 10 cm inter-microphone spacing; the diameter of the sphere on which the microphones lie is not the same across all designs, however. Designing the arrays to have the same intermicrophone spacing ensures they'll have similar upper frequency cutoffs (where spatial aliasing becomes a problem). In all cases the steering direction (indicated by the "+" symbol) is through the centre of one of the faces defining the polyhedron. Different performance will be found by steering the array in different directions. Panel (b) shows the beam pattern at 1 kHz for the optimized design (solid curve) and for a uniformly-weighted (delay-and-sum) beamformer with the same geometry (broken curve). The patterns are shown in the plane containing the centre of the array, the steering direction indicated in panel (a), and one of the microphones defining the face through which the array is steered. The steering direction is at 0°. Panel (c) is a plot of the directional gain versus frequency for the optimized design (solid curve) and the delay-and-sum design (broken curve). Panel (d) is a plot of the white noise gain, for the optimized design (solid curve) and the delay-and-sum design (broken curve).

Notice that the directional gain curves for the optimized designs are higher than for the delay-and-sum designs, but that the white noise gain curves

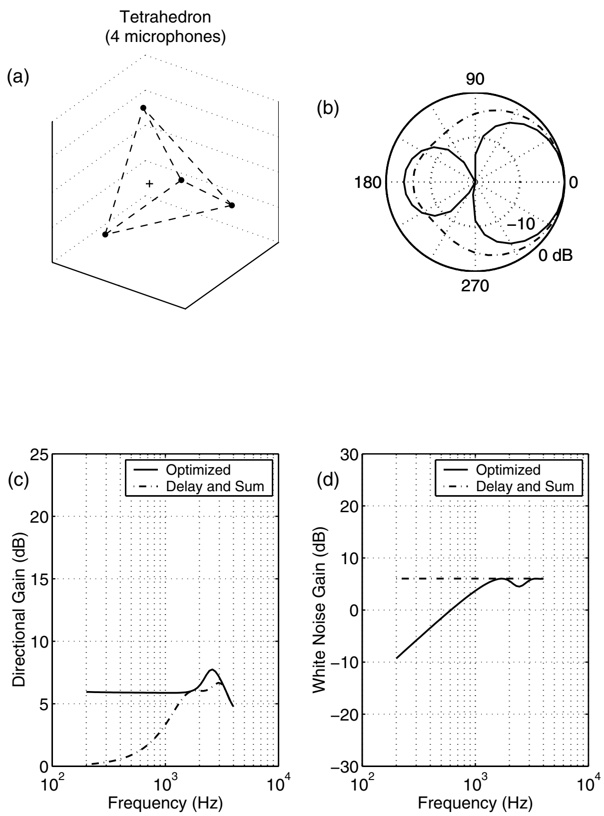

Fig. 4: Tetrahedral array designed assuming 0.1 dB sensor noise. (a) Array geometry (sphere diameter 12.2 cm, microphone spacing 10 cm), (b) 1 kHz beam pattern for optimized design (solid curve) and delay-and-sum design (broken curve), (c) directional gain for optimized design (solid curve) and delay-and-sum design (broken curve), and (d) white noise gain for optimized design (solid curve) and delay-and-sum design (broken curve).

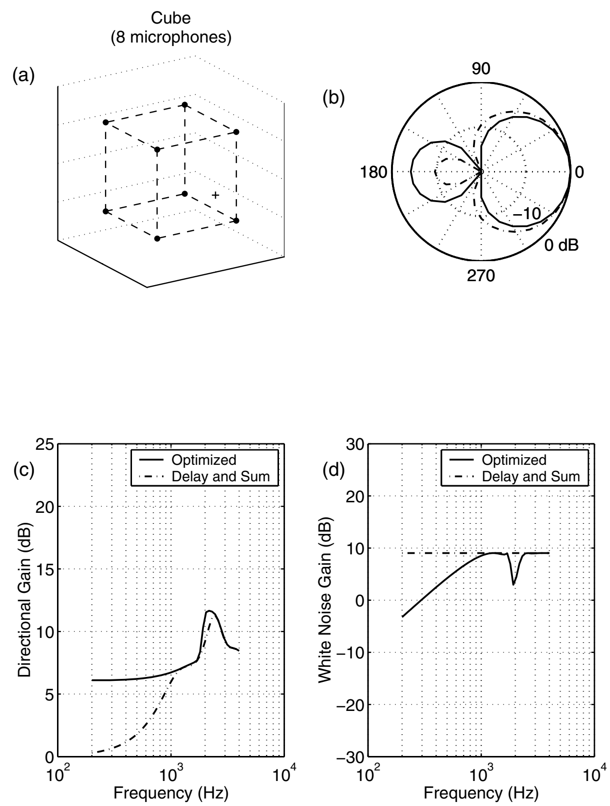

Fig. 5: Cubic array designed assuming 0.1 dB sensor noise. (a) Array geometry (sphere diameter 17.3 cm, microphone spacing 10 cm), (b) 1 kHz beam pattern for optimized design (solid curve) and delay-and-sum design (broken curve), (c) directional gain for optimized design (solid curve) and delay-and-sum design (broken curve), and (d) white noise gain for optimized design (solid curve) and delay-and-sum design (broken curve).

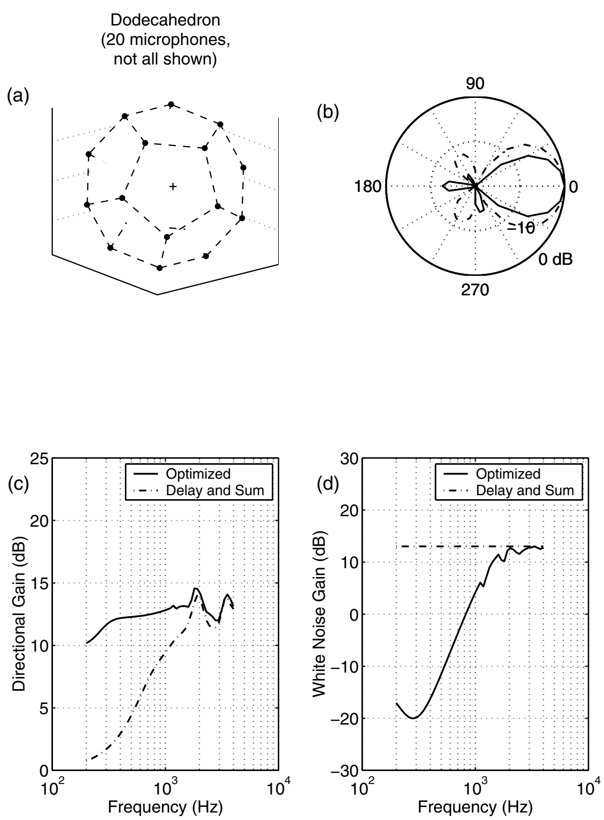

Fig. 6: Dodecahedral array designed assuming 0.1 dB sensor noise. (a) Array geometry (sphere diameter 28.0 cm, microphone spacing 10 cm) microphones on back half of array not shown, (b) 1 kHz beam pattern for optimized design (solid curve) and delay-and-sum design (broken curve), (c) directional gain for optimized design (solid curve) and delay-and-sum design (broken curve), and (d) white noise gain for optimized design (solid curve) and delay-and-sum design (broken curve).

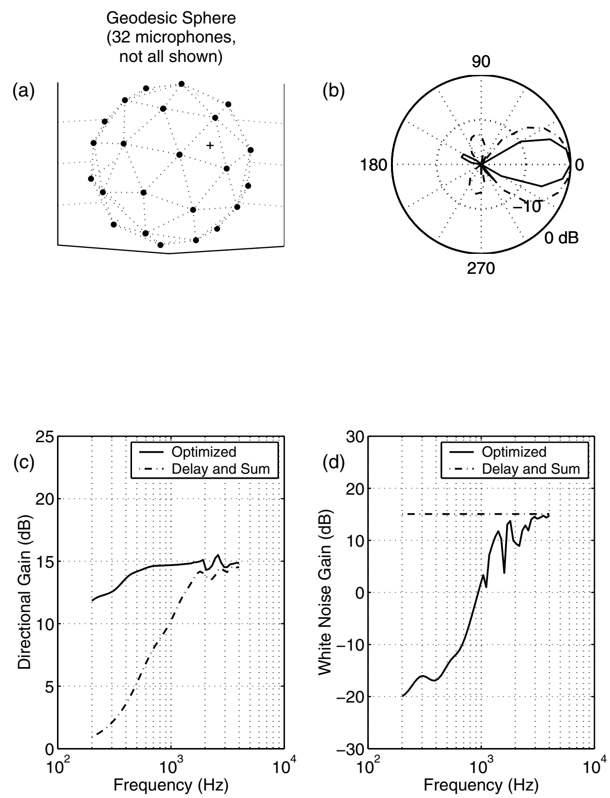

Fig. 7: Geodesic array designed assuming 0.1 dB sensor noise. (a) Array geometry (sphere diameter 31.2 cm, microphone spacings 10 cm and 11.1 cm), microphones on back half of array not shown, (b) 1 kHz beam pattern for optimized design (solid curve) and delay-and-sum design (broken curve), (c) directional gain for optimized design (solid curve) and delay-and-sum design (broken curve), and (d) white noise gain for optimized design (solid curve) and delay-and-sum design (broken curve).

are lower. Some of the ability of the array to reject noise (i.e., robustness) has been traded off in favour of higher directional gain. Also notice that the performance of each array drops off at low frequencies, and becomes erratic at high frequencies. These are results of the signal-to-noise problems (at low frequencies) and of spatial aliasing (at high frequencies). The notches and dips in the white noise gain curves are presumed to be manifestations of having an incomplete basis from which to form a high-order beam—they can be avoided by adding or moving microphones off the spherical surface or by constructing the array in a rigid body, for instance [22]. Another approach is to smooth the white noise gain curve and perform a second design step using this smoothed curve as a target [12]. This is the approach used in the design described in the next section.

The geodesic sphere array design achieves a directional gain of 14 dB, which is comparable to the target identified above from the simulations.

4. ARRAY CONSTRUCTION

Based on the above, a geodesic sphere array was constructed. The array has a diameter of 48 cm and is intended to operate over the frequency band of 300–1000 Hz. This array is described in Refs. [12, 23], along with a 16 cm similar array designed to operate over 1000–3300 Hz.

A photograph of the 48 cm array is shown in Fig. 8. The stand is constructed from 2.4 mm stainless steel rods, arranged like “spokes” sticking out of a central shaft. The shaft is supported by 4 thin steel legs, which are used to carry the microphone cables. The microphones are 6 mm omnidirectional electrets (Panasonic WM-61A102B) and are held in place by taping the cables to the spokes. The microphone capsules are not actually touching the stand.

The beamforming filters were designed for a microphone noise level of 0.1 dB. This was determined by measuring a large number of microphone responses in an anechoic chamber, and selecting a set of 32 that were closely-matched. Figure 9 shows the 32 microphone responses, each normalized by their average and shifted by their mean sensitivities. That is, the plot shows the residual differences in the microphone responses, after applying a gain correction to each. The standard deviation of magnitude is at

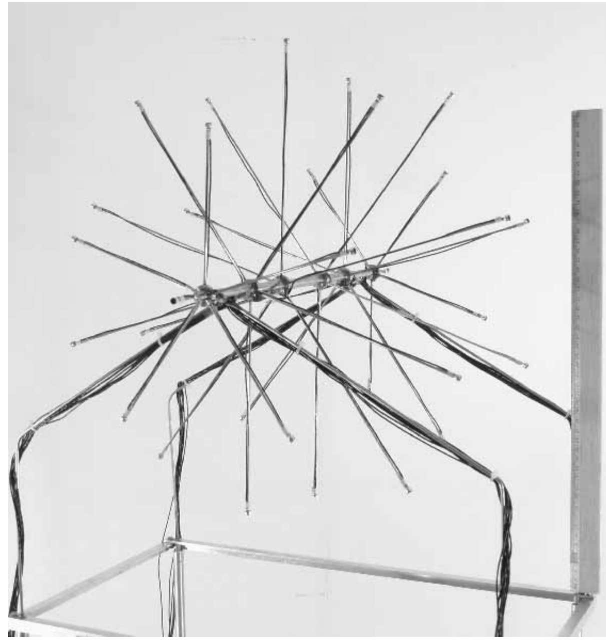

Fig. 8: Photograph of 48 cm geodesic spherical array with 50 cm ruler.

worst 0.1 dB and that of phase is at worst 0.5° over 300–1000 Hz.

The beam pattern of the array, computed from the beamforming filters is shown in Fig. 10. The figure shows the average beam pattern over 300–1000 Hz, in the plane containing the centre of the array, the steering direction (through the centre of one of the 60 triangular faces), and one of the microphones bounding that face. The beamwidth is 28°, which is comparable to the sixth-order hypercardioid, although the sidelobes are higher (refer to Fig. 2; notice the different scales). The pattern is asymmetric since the array is asymmetric in this plane. The response of the array is identical in the directions through the other 59 triangular faces. (These 60 steering directions are 22° or 24° apart.)

5. EXAMPLE MEASUREMENT

The 48 cm geodesic sphere array was used to measure the sound field in a small videoconferencing room. A computer equipped with an 8-channel sound card (Echo Audio Layla24) was used to play a maximum-length-sequence (MLS) over an omnidirectional loudspeaker while simultaneously record-

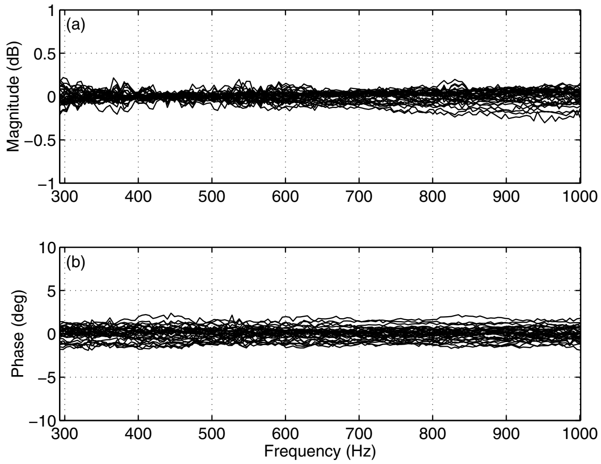

Fig. 9: Residual responses of 32 microphones used in construction of geodesic sphere array (a) magnitude, (b) phase. Microphone responses have been normalized by their average, and shifted by their individual sensitivities.

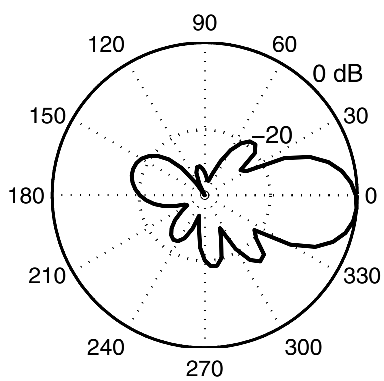

Fig. 10: 48 cm geodesic spherical array beam pattern in a plane containing the centre of the array, the centre of a triangular face, and one microphone defining this face. This is the average beam pattern over 300–1000 Hz.

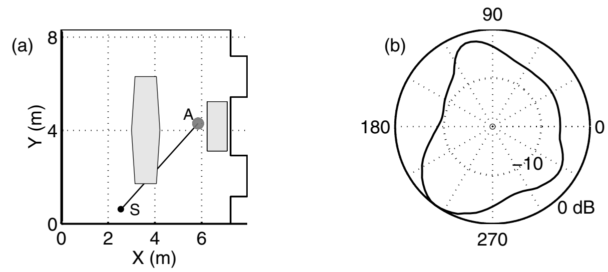

Fig. 11: Measurement with 48 cm geodesic spherical array. (a) Top view of room showing source position (S), array position (A), a table, and a cabinet. (b) Top view of arriving energy integrated over full time decay of room, including direct sound. The direct sound arrival (at 235°) and the reflection from the far wall (at 110°) are evident.

ing 8 of the array microphones. This process was repeated until all 32 array microphones were sampled, then the microphone recordings were processed to generate a set of 32 omnidirectional room impulse responses. These RIRs were beamformed to generate a set of 60 directional room impulse responses—the response of the array in the 60 steering directions. The level in each steering direction was computed by integrating the directional responses over the full time of decay of the room.

The results are shown in Fig. 11. Panel (a) of the figure shows a top view (plan view) of the room, indicating source (S) and array (A) positions. Panel (b) shows a plot of the incident energy at the array, viewed from the same perspective. The peak sound arrival directions of 235° and 110° agree with the expected direct sound and back wall reflections, computed from the room geometry.

By integrating the impulse responses over different time windows, or by inspecting them instantaneously, the temporal evolution of the sound field can be examined. The arrival direction and time of specular reflections can be found. Also, overall assessments of the diffuseness or isotropy can be made. More detailed discussions of measurements made with this array are described in Refs. [12, 23, 24].

6. CONCLUSIONS

Spherical microphone arrays are well-suited to analysis of directional information in sound fields. Powerful computers and inexpensive microphones and sound cards are making it possible to realize sophisticated arrays, so frequently the problem comes back to design. A design approach of defining requirements, selecting candidate geometries and beamformer design procedures, then evaluating the designs was used to arrive at a 32-element geodesic sphere array. After careful selection of microphones, the array was constructed and used for room acoustical measurements. Directions of important sound incidence were easily identified in a small room. In areas such as room acoustic characterization or diagnosis, source and reflection detection, leak detection, flanking path identification, and diffuse field assumption validation, it is anticipated that directional arrays can be quite useful.

7. ACKNOWLEDGMENTS

BNG would like to thank Dr. John Vanderkooy at the University of Waterloo (Ontario, Canada) for many useful technical discussions, and for financial support.

8. REFERENCES

[1] R. Thiele, "Richtungsverteilung und Zeitfolge der Schallrückwurfe in Räumen," Acustica **3**, 291–302 (1953).

[2] A.D. Broadhurst, "An acoustic telescope for architectural acoustic measurements," Acustica **46**, 299–310 (1980).

[3] H. Tachibana, Y. Yamasaki, M. Morimoto, Y. Hirasawa, A. Maekawa, and C. Pösselt, "Acoustic survey of auditoriums in Europe and Japan," J. Acoust. Soc. Jpn. (E), **10**, 73–85 (1989).

[4] A. Abdou and R.W. Guy, "Spatial information of sound fields for room-acoustics evaluation and diagnosis," J. Acoust. Soc. Am. **100**, 3215–3226 (1996).

[5] H. Okubo, M. Otani, R. Ikezawa, S. Komiyama, and K. Nakabayashi, "A system for measuring the directional room acoustical parameters," Appl. Acoust. **62**, 203–215 (2001).

[6] T. Peltonen, T. Lokki, B. Gouatarbès, J. Merimaa, and M. Karjalainen, "A system for multichannel and binaural room response measurements," Convention Paper 5289, Presented at the 110th Convention of the Audio Engineering Society, Amsterdam, 12–15 May (2001).

[7] J. Merimaa, T. Lokki, T. Peltonen, and M. Karjalainen, "Measurement, analysis, and visualization of directional room responses," Convention Paper 5449, Presented at the 111th Convention of the Audio Engineering Society, New York, 21–24 September (2001).

[8] W. Täger and Y. Mahieux, "Reverberant sound field analysis using a microphone array," Proceedings ICASSP-97, IEEE International Conference of Acoustics, Speech, and Signal Processing, Munich, Germany, April (1997).

[9] J.S. Abel and D.R. Begault, "Methods for room acoustic analysis using a monopole-dipole microphone array," Proceedings InterNoise98, Paper 123. International Congress on Noise Control Engineering, Christchurch, New Zealand, November (1998).

[10] D.I. Havelock, G.A. Daigle, and B.N. Gover, "Localization of noise source and primary reflections in a room using a spherical array and aggregate beamforming technique," Paper N275, Presented at Inter-Noise2003, Seogwipo, Korea, 25–28 August (2003).

[11] T. Nishi, "Development of a multi-beam array microphone for multi-channel pickup of sound fields," Acustica **76**, 163–172 (1992).

[12] B.N. Gover, J.G. Ryan, and M.R. Stinson, "Microphone array measurement system for analysis of directional and spatial variations of sound fields," J. Acoust. Soc. Am. **112**, 1980–1991 (2002).

[13] G.W. Elko, "Superdirectional Microphone Arrays," Chapter 10 of *Acoustic Signal Processing for Telecommunication*, edited by S.L. Gay and J. Benesty (Kluwer Academic, Norwell, MA, 2000).

[14] J.B. Allen and D.A. Berkley, "Image method for efficiently simulating small-room acoustics," J. Acoust. Soc. Am. **65**, 943–950 (1979).

[15] D.H. Johnson and D.E. Dudgeon, *Array Signal Processing: Concepts and Techniques*, (Prentice-Hall, Englewood Cliffs, NJ, 1993).

[16] J.L. Flanagan, "Use of acoustic filtering to control the beamwidth of steered microphone arrays," J. Acoust. Soc. Am., **78**, 423–428 (1985).

[17] G.W. Elko, "Microphone array systems for hands-free telecommunication," Speech Communication, **20**, 229–240 (1996).

[18] D.K. Cheng, "Optimization techniques for antenna arrays," Proc. IEEE, **59**, 1664–1674 (1971).

[19] M.R. Stinson and J.G. Ryan, "Microphone array diffracting structure," Canadian Patent Application CA-2292357 (1999). Available on-line at `http://patents1.ic.gc.ca`

[20] H. Cox, R.M. Zeskind, and M.M Owen, "Robust adaptive beamforming," IEEE Trans. ASSP, **35**, 1365–1376 (1987).

[21] J.G. Ryan and R.A. Goubran, "Optimum near-field performance of microphone arrays subject to a far-field beampattern constraint," J. Acoust. Soc. Am., **108**, 2248–2255 (2000).

[22] J. Meyer, "Beamforming for a circular microphone array mounted on spherically shaped objects," J. Acoust. Soc. Am., **109**, 185–193 (2001).

[23] B.N. Gover, "Development and use of a spherical microphone array for measurement of spatial properties of reverberant sound fields," Ph.D. thesis, Department of Physics, University of Waterloo, Waterloo, Canada (2001).

[24] B.N. Gover, J.G. Ryan, and M.R. Stinson, "Measurements of directional properties of reverberant sound fields in rooms using a spherical microphone array," submitted to J. Acoust. Soc. Am. (2003).